Structure and properties of metal-free conductive tracks on polyethylene/multiwalled carbon nanotube composites as obtained by laser stimulated percolation

(Article begins on next page)

03 May 2024

Structure and properties of metal-free conductive tracks on polyethylene/multiwalled carbon nanotube composites as obtained by laser stimulated percolation

Federico Cesano[a§], Ismael Rattalino[b§], Danilo Demarchi[b], Fabrizio Bardelli[a], Alessandro Sanginario[b], Annamaria Gianturco[c], Antonino Veca[c], Claudio Viazzi[d], Paolo Castelli[d], Domenica Scarano[a], and Adriano Zecchina[a]*

[a] Department of Chemistry and NIS (Nanostructured Interfaces and Surfaces) Centre of Excellence and INSTM Centro di Riferimento, University of Torino, Via P. Giuria, 7, 10125 Torino (Italy);
[b] Department of Electronics and Telecommunications, Politecnico di Torino, Corso Duca degli Abruzzi 24, 10129 Torino (Italy);
[c] Centro Ricerche Fiat S.C.p.A., Str. Torino 50, I-10043 Orbassano (Italy);
[d] RTM Laser Technology SpA, Via Circonvallazione 10, I-10011 Agliè (Italy);
[§] these authors contributed equally to this work.

Abstract

The fabrication and characterization of conductive tracks by laser irradiation on non-conductive multiwalled carbon nanotube/polyethylene (MWCNT/HDPE) composites is reported. Along the irradiated paths the percolation of MWCNTs is occurring, as demonstrated by field emission scanning electron and atomic force microscopies. An increment of tracks conductivity of several orders of magnitude is documented by single pass Kelvin probe force and current sensing atomic force microscopies, together with electrical measurements. The structure of conductive paths has been estimated by secondary electron charge contrast imaging.

The investigation has been developed from basic characterization up to industrial scale manufacturing. The method is fast, flexible and innovative, because: i) highly adherent tracks of any selected pattern on a low cost material can be obtained, ii) the tracks are metal-free, a fact rendering the composite fully recyclable and iii) the irradiated materials have application for electrical signals transport; iv) the tracks are also characterized by piezoresistive properties so allowing their employment as pressure sensors.

* Corresponding author. Tel: +39 0116707860. Fax: +39 0116707855. E-mail address: adriano.zecchina@unito.it (A. Zecchina)

1. Introduction

Composites materials based on conducting fillers such as metal particles, carbon nanotubes (CNTs), carbon nanofibers (CNFs) and graphene, dispersed in insulating polymeric matrices are attracting a considerable interest for their use in polymeric and flexible electronics, anti-static and electromagnetic interference shielding, sensing and structural applications [1-11].

Due to the excellent electric properties of CNTs [12], CNT/polymer composites have been extensively investigated and low density polyethylene (LDPE), high and ultra high density polyethylene (HDPE and UHMWPE) have been used as matrices [13]. The resulting electric properties are mainly determined by filler concentration. Composites characterized by filler concentration lower than ≈0.5−5 wt% are characterized by very low conduction while composites with concentration higher than the percolation threshold (i.e. the concentration associated with the formation of a continuous net of CNTs), are characterized by conductivity several order of magnitude larger.

In particular, considerable efforts have been made on the fabrication of conducting tracks based on metals (e.g. Ag) and/or carbon [7, 14-16], doped polymers (e.g. polyacetylene, polythiophene, pentacene, etc.) [17] on non conducting matrices.

As for conductive tracks obtained by thermal treatment of low concentrated CNT/polymer matrices, primarily constituted by immiscible polymer blends and containing CNTs in low amount and additives, information was first reported in an exhibition fair [18] and in a patent [19]. According to these reports, upon thermal heating by means of a wide range of methods including laser treatment, the nonconductive surface of CNT/polymer blends loaded with additives is becoming conductive. In these reports no detailed information about the structure and properties characterization at micro-nano level of the produced systems is reported. For sake of completeness, it is useful to recall that the laser writing technique has also proved its utility for in-situ localized reduction of graphite oxide [16].

In this paper, we describe the formation of conductive paths obtained by CO_2-pulsed laser irradiation (laser writing) of the surface of multiwalled carbon nanotubes (MWCNTs)/polymer composites constituted by a single polymer phase (high density polyethylene, HDPE) and MWCNTs with concentration ranging in the 0.5-5 wt% interval. No additives and additional phases are present in our system, which so appears ideal for a basic investigation at the micro/nano level of the laser induced percolation process and on the structure of the conductive tracks. It will be shown by means of several techniques that in the regions stimulated by the laser beam, polymer melting is induced together with the formation of an accumulation layer, where the percolation of nanotubes is occurring. This leads to the formation of tracks characterized by an enhancement of conductivity of several orders of magnitude. The obtained tracks are stable because the accumulation layer is firmly adhering to the undisturbed polymer phase. This result is highly relevant because a selective control of the conductivity along tracks of any selected pattern, surrounded by an insulating bulk, is important in many industrial applications, where the dispersion of the electric signal through the composite must be avoided.

2. Materials and methods

2.1. Material preparation.

The carbon nanotubes used in this work were previously and extensively characterized in other papers [20, 21]. The CNTs are highly-crystalline multiwalled carbon nanotubes, 10–15 µm in length and with external diameters of 30–90 nm. The high-cristallinity and purity of the material are confirmed by Raman spectroscopy and AE-ICP spectrometry (Fe 0.61 ± 0.01, Al 0.04 ± 0.05, Ni 0.003 ± 0.001). MWCNTs/polymer composites were prepared by the melt compounding of High Density Polyethylene (HDPE) in a mixer with counter rotating screws (Brabender). CNT/polymer composites with different amounts (0.5-5 wt%) of multiwalled-carbon nanotubes (MWCNTs, Mitsui) were obtained by adding portions of MWCNTs to the HDPE polymer in the chamber at 180°C under a rotation speed of 50 rpm. The mixing was stopped after 5 min to limit the oxidation of the polymer phase. Final materials were then remoulded at the mixing temperatures and pressed for 10 min under 100 bars of pressure to gain flat samples 3 mm thick.

2.2. Laser processing.

The equipment consists in a laser CO_2 (λ=10.6 µm, El-En Blade 1500) equipped with scanning heads and focusing optics with a power of several W operating either in continuous (CW) or in pulsed emissions. This allows an easy generation of a complex path on the sample with tracks of different widths (using wobble for larger tracks), lengths, and geometries. Linear laser speeds in the 9-2000 mm/s interval have been tested under a coaxial flow of N_2. The best results were obtained by using 32Wpower, 9 mm/s scanning speed and 30L/min N_2 flow at atmospheric pressure.

2.3. Material characterization.

The morphology of the samples has been investigated by means of: i) field emission scanning electron microscopy (FESEM, ZEISS SUPRA 40) equipped with a field emission tungsten cathode and an energy dispersive X-ray detector, ii) atomic force microscopy (AFM, Park Systems XE-100). Before FESEM and AFM analyses, the samples were preventively cryo-fractured and chemically etched by a $KMnO_4/H_3PO_4/H_2SO_4$ etching treatment for 15h.

Raman spectra on unperturbed and on laser treated regions were obtained by a Renishaw inVia Raman Microscope, laser line 514 nm, 20x ULWD objective (power at the sample < than 1mW).
Cross-sections conductivity profiles of the laser irradiated regions were obtained by a secondary electron (SE) detector of a Zeiss Evo50 SEM operating at low potential of acceleration (0.3-0.5KeV), on samples specifically prepared. More in details, the secondary-electrons edge effects (morphology) of samples were reduced by working on "flat" sections of material obtained by means of the ultramicrotome technique usually adopted for transmission electron microscopy sample preparation: i) by embedding the sample in epoxy resin to fill voids in order to constitute a block, which is then cross sectioned, ii) by using a regular gem-

grade diamond knife. Microtome slices 0.1-1 µm in thickness representing the cross-section area of the laser irradiated regions along its length were obtained from the block material. Samples were then investigated by phase-contrast low voltage SEM on either, block and cut slices, which were contacted on the back sides with conductive Ag paste suitable for AFM conductive imaging as well. Due to the more regular and flat surface, better results were obtained on the cut block surface of materials.

Topography and surface potential maps were obtained by single-pass Kelvin probe force microscopy (SKPFM) in the intermittent contact mode by using an Agilent 5500 Scanning Probe Microscope with a 100µm xy-scanner range, operating in acoustic AC mode for Kelvin probe force microscopy (KFM) in single-pass mode. Topography, current and resistance maps were obtained by current sensing atomic force microscopy (CSAFM) by using an Agilent ResiScope module connected with an Agilent 5500 Scanning Probe Microscope for simultaneously probing the conductivity and topography. The Agilent ResiScope allows to measure a wide range of resistances (0.1KΩ - 1TΩ) and currents (1mA - 100fA). The resistance and current can be either in linear or in the log-scale outputs.

Images were acquired on cross sections of samples taken at the boundary of the laser-irradiated regions with the embedding epoxy resin. The post-processing of acquired images was carried out by using Agilent PicoImage software.

The electrical measurements were obtained on tracks with typical lengths in the 50-100 mm interval. Before the electric characterization, Au electrodes have been deposited onto the two endings of tracks by vacuum sputtering. A Keithley 6430 Sub Femto Amperometer SourceMeter was used for low current electrical characterization (up to 100 µA). Low current measurements were performed in a metal box (Faraday cage) under nitrogen atmosphere in glove box. An Agilent N5752A System DC Power Supply was used for higher current electrical characterization (up to tens of mA). An Agilent 4294A Precision Impedance Analyzer was used for electrical characterization upon frequency. An Angelantoni TY 80 climatic system was used for electrical characterization upon temperature. The electric conductivity cross-sections have been obtained from conductivity maps estimated by SEM images performed in contrast mode, where the conductive sections (bright region) are clearly delimited by a strong difference in the contrast of the image.

A set up to qualitatively investigate the piezoelectric properties of the tracks has been constructed.

3. Results and discussion
3.1. *The laser printing methodology and the morphological modifications.*
The tracks have been produced under controlled atmosphere by means of a focalized laser beam impinging on the surface of composites plates containing a variable concentration of carbon nanotubes. The scheme of the laser manifold is illustrated in Fig. 1a, while details concerning the preparation and the structure of the composites with concentration ranging in the 1-5 wt% interval are reported in Supplementary data**.** The effect of the laser beam is the localized melting of the polymer phase with formation of a v-shaped channel (Scheme in Fig. 1a).
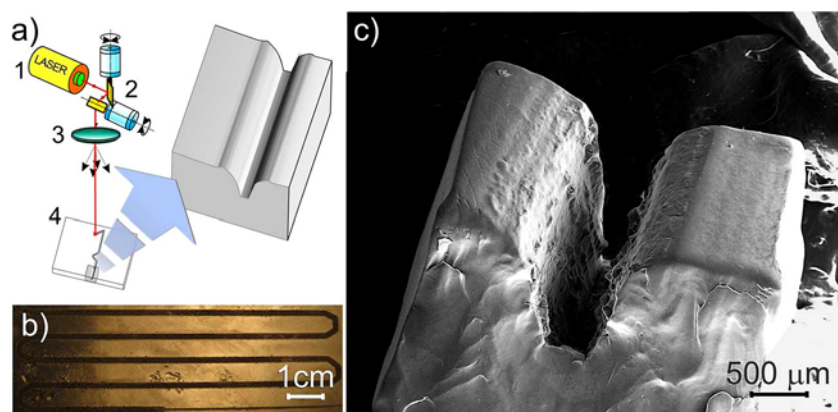
Fig. 1. a) The material processing device: 1 Laser beam source, 2 mirrors, 3 lenses and 4 sample. Mirrors and lenses, are necessary to focalize the laser beam on the sample. A scheme of a magnified laser-irradiated area with formation of a v-shaped channel profile is shown in the right part of a); b) photo of a sample in a region showing a square waveform pattern several cm long, as obtained by single-pass or dual-pass laser processing; c) typical SEM lateral view at low magnification of the v-shaped track just after the laser treatment. Floating MWCNT are not yet removed by gentle brushing.

Among all the attempted approaches (i.e. laser sources, continuous or modulated emissions, writing speed, inert atmosphere or air, etc.) the processing using CW CO_2 laser emitting in the IR range has been found very effective, fast and reproducible so allowing the versatile industrial-scale manufacturing of conductive tracks with complex geometries on low concentrated CNT/polymer composites. An example of the laser processing of HDPE/CNT composite is shown in Fig. 1b. The morphology of the track is well evidenced in the SEM image shown in Fig. 1c. It is inferred that, due to the thermal effect of the laser beam, the melted polymer phase formed in the irradiated region is partially accumulated at the borders of the track with formations of symmetric hills of amassed material. It will be shown in the following that the concentration of MWCNTs originally occupying the removed matrix volume, is increased at the borders of the V-shaped channels because of formation of CNTs "accumulation layer". It is noteworthy that few floating CNT residues of the original matrix can remain in the channel as imaged in Fig. 1c. These residues can be easily removed by gently brushing the plate.

3.2.   The structure of composites before and after laser irradiation.
The structure of the composites before irradiation is illustrated in Fig. 2a-c. From SEM images, the growing concentration of carbon nanotubes emerging from the HDPE matrix on passing from 1wt% to 5wt% samples, can be appreciated. The number of "interconnections" among CNTs increases with the filler loading. From the SEM images, the presence even at highest loading (5 wt%) of a continuous net of interconnected CNTs, cannot be inferred. This is a clear indication that before irradiation, 5 wt% samples prepared following our simplified procedure show insulating properties (*vide infra).*
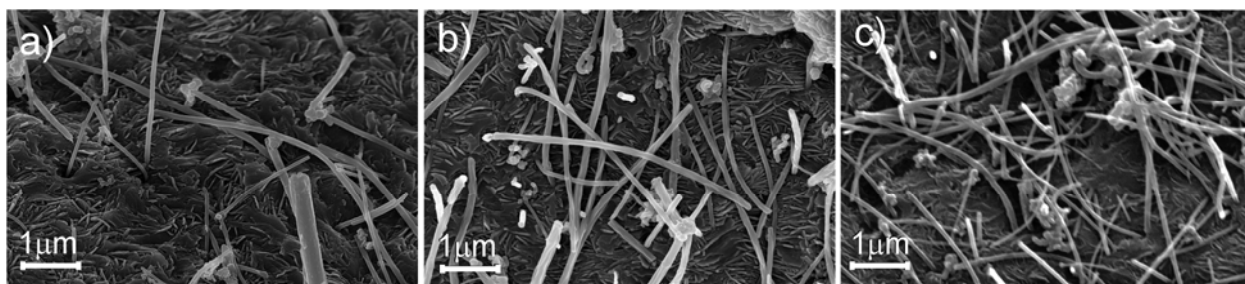
Fig. 2. a): morphology of HDPE/MWCNT composites at increasing MWCNT concentration, as obtained by SEM: a) 1 wt%, b) 3 wt% and c) 5 wt%. The SEM images have been obtained on chemically etched surfaces of cryo-fractured samples. Permanganic/ortophosphoric/sulphuric chemical etching of the surface material has been adopted to better image the microstructure of the samples [22].

The structure of the composites after laser irradiation is illustrated in Fig. 3. The high resolution SEM image of a part of the v-shaped track in a 3 wt% sample, where both the unperturbed matrix and the "accumulation border region" are present, shows that the CNT concentration is greatly increased in the accumulation region with respect to the bulk (Fig. 3a). This conclusion is confirmed by the exploded views reported in Fig. 3b,c and by Raman spectra illustrated in Fig. 4.
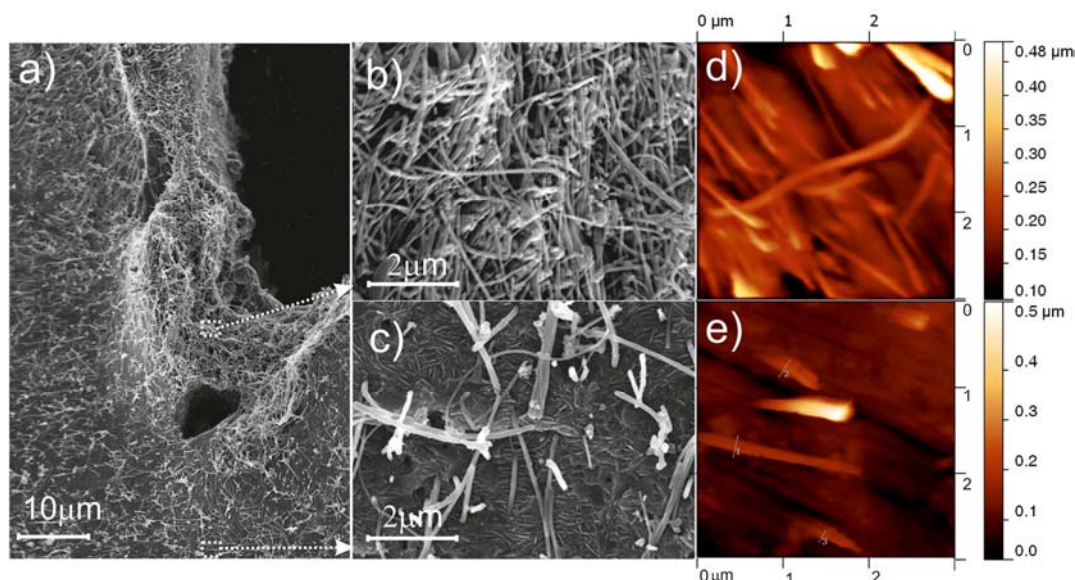
Fig. 3. a) SEM lateral view of a laser-irradiated region of 3 wt% composite; b) and c) high-resolution SEM images taken along the profile of the track and in a region far from the laser track, respectively; d) and e) AFM images of the same regions shown in b) and c). From these images, it is clearly inferred that the CNTs concentration is greatly increased in the accumulation layer, where percolation and formation of a continuous network are occurring as demonstrated (*inter alia*) by electrical measurements.

In this figure, Raman spectra of MWCNT/HDPE composite with 3wt% of MWCNTs are specifically described because they can be considered to have prototype character. The most relevant conclusions are: a) in the spectra obtained along the tracks (where the MWCNTs

concentration is high and they are forming a electrically connected network) the G, G', D peaks of the MWCNTs are dominating, while the classical bands of PE in the 1500-1000 cm^{-1} region are hardly visible while those in the 2800-2950 cm^{-1} range are severely weakened. In other words the MWCNT spectrum is obscuring that of the PE matrix as expected. A more detailed discussion of these fingerprints (D, G, G'-bands) is beyond the scope of this paper and can be found elsewhere [23, 24]. The peaks located at 2849cm^{-1} and at 2885 cm^{-1} are the symmetric and antisymmetric CH$_2$ stretching modes of the polymer phase [25]; b) in the spectra taken in the unperturbed region, beside the G, G' and D bands of MWCNTs, the classical peaks of PE are clearly visible also in the 1500-1000 cm^{-1} range which are assigned to CH$_2$ bendings and twisting (1421 cm^{-1}, 1357 cm^{-1}, 1296 cm^{-1}), and C-C stretchings (1063 cm^{-1} and 1130 cm^{-1}) [26]. This result is the expected one because the less densely concentrated MWCNTs are not shielding Raman spectrum of the polymer. For the same reason also in the high frequency region (2800-1950 cm^{-1}) the intensity of the PE peaks is remarkable. Only one feature merits a specific comment: it is concerning the 2885 cm^{-1} peak which looks more prominent. As a similar phenomenon is observed on PE films oriented with respect to the laser beam [27], we think that, due to lamination and compression effects used in the preparation of the samples in the unperturbed regions, the polymer chains are not randomly oriented.

As for the other concentrations are concerned, the following can be summarized: a) for MWCNTs concentration lower than 3% the PE bands are always clearly visible in all ranges; b) for MWCNT concentration higher that 3wt% the spectra are dominated by the G, G' and D-bands while those of PE are hardly visible.

The formation of a V-shaped track with formation of a MWCNT accumulation layer on the external walls is the results of many concurrent and complex effects.

Among all the following can be mentioned:

a) under the effect of the laser beam the localized melting of the polymer phase is occurring , with formation of a viscous liquid.

b) under the action of the N$_2$ flow, which is impinging the composite surface along the same direction of the laser beam, the liquid phase is moving away and become amassed on the external periphery of the track with formation of accumulation hills, well illustrated in the SEM images (Fig. 3a,b,d).

c) the temperature of the melted phase is not homogeneous: it is maximum at the centre of the track and decreases at the borders. The same occurs for the MWCNTs mobility (which so tend to accumulate at the colder borders),

d) as the viscosity of the melted phase decreases with the CNTs decreasing concentration, it is expected that the liquid phase, more rapidly moving away, is containing a smaller fraction of CNTs.
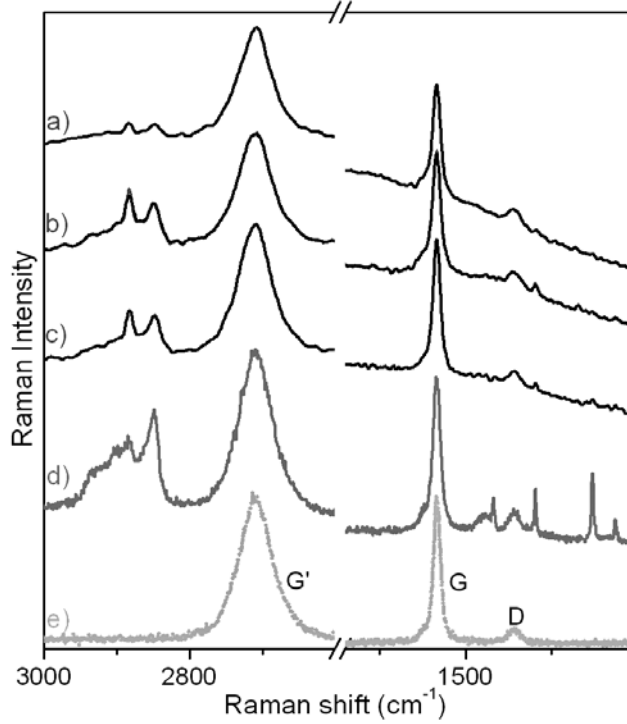
Fig. 4. Raman spectra of the MWCNT/HDPE polymer composite (3wt% of MWCNTs) obtained on different selected regions: a-c) spectra obtained on the conductive track and d) spectra obtained on an unperturbed region (bulk); e) spectra of pristine MWCNTs.

The effects c) and d) are well known, as reported in refs [28, 29].

A qualitative comparison with Fig. 2, allows to conclude that the concentration of MWCNTs in the accumulation layer is definitely higher than 5 wt%, so showing that the percolation threshold has been reached [30]. AFM images (Fig. 3d,e) confirm the results obtained by SEM. Analogous data (not shown for brevity) have been obtained for the other investigated compositions (1 wt% and 5 wt%).

In conclusion on the basis of the previous points, at high MWCNT content, characteristic of the borders of the V-shaped channel, CNTs are expected to entangle together to form a more interconnected structure, characterized by tunnelling electric properties [28].

3.3. Electric properties.

The formation of accumulation layers, where CNTs are forming a dense interconnecting network, is associated with increased electrical conductivity with respect to the pristine material. This has been qualitatively highlighted on 3 wt% sample by means of secondary electrons charge-contrast imaging (Fig. 5a), by Single Pass Kelvin Probe Force and by Current Sensing Atomic Force Microscopies (Fig. 5b,c, respectively).

The dark regions of Fig. 5a obtained by secondary electron imaging refer to the non-conductive regions of the epoxy resin used to fill the void parts of the v-shaped track and to MWCNTs/HDPE portions of the sample not involved by the laser irradiation. The bright region refers to the accumulation layer, where the MWCNT concentration is beyond the percolation threshold and hence, is behaving as an electric conductive region. The thickness of the conductive accumulation layer, as appreciated from the inset of Fig. 5a, is about 20μm.

9

The results obtained by Kelvin Probe Force Microscopy (Fig. 5b) confirm that a huge potential difference is present at the boundary between the low conducting epoxy region and the conductive accumulation layer. Images obtained with AFM equipped with a Resiscope device (Fig. 5c) are in full agreement. Similar data have been obtained on the 5 wt% sample.
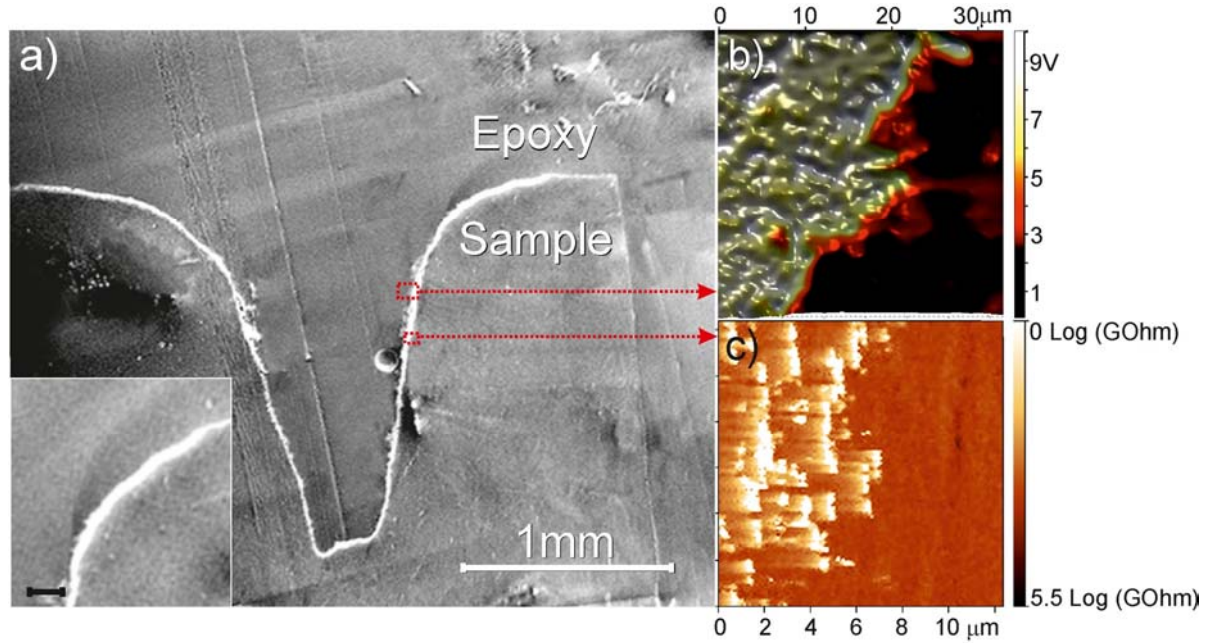
Fig. 5. a) SEM image of the cross section (obtained with ultramicrotome technique) of 3%wt sample, as obtained by means of secondary electrons in voltage-contrast imaging mode under low acceleration voltage (0.3 KeV) [31, 32]. Edge effects are reduced by embedding the sample in the epoxy resin. Dark regions refer to non-conductive regions (epoxy resin or matrix portions not perturbed by irradiation), whereas the bright region refers to the electric conductive area (accumulation layer). In the inset of a) a magnification of the accumulation layer is shown. Scale-bar is 100µm.
b) Surface potential scan (32x32µm) obtained by Single Pass Kelvin Probe Force Microscopy, acquired at the boundary between the laser-irradiated region and the embedding epoxy resin.
c) Direct resistance atomic force map of the boundary region between the track and the unperturbed composite material shown in a) as obtained by using the AFM equipped with Resiscope device.

In order to further investigate the electrical properties of the conductive tracks, AC and DC electrical characterizations were performed on the samples with CNT concentrations in 1−5 wt% range, before and after laser irradiation. Fig. 6a,b compare the DC electrical behaviour of untreated and irradiated regions of the 5wt% CNT sample, considered as representative of all the filler concentrations. It is evident that the samples are conductive inside the tracks (from 6 to 12 Ω cm), whereas they are insulating (more than 200 GΩ cm), anywhere in the bulk or in the surface portions not treated with the laser beam. The same result is qualitatively evidenced by the maps of conductivity. Notice that after brushing the surface and cleaning with acetone, the tracks conductivity is lowering at most of the 10-15% and then remains stable. The current

10

density and resistivity versus the electric field plots were obtained following the geometrical scaling procedure described in Supplementary data.

Irradiation causes an enormous decrease in resistivity (around 11 orders of magnitude), and the transition from a non-linear (quasi-quadratic) to a linear dependence of the resistivity and of the current density on the applied voltage. The non-linear behavior observed before irradiation is that expected for polymer-CNT composites under percolation threshold, [33, 34] where the transport mechanism is governed by the tunneling effect.

Conversely, over percolation threshold a continuous net of CNTs is formed without gaps in the electron pathways, resulting in a linear conductive behaviour, which follows the classic Ohm law. [30]
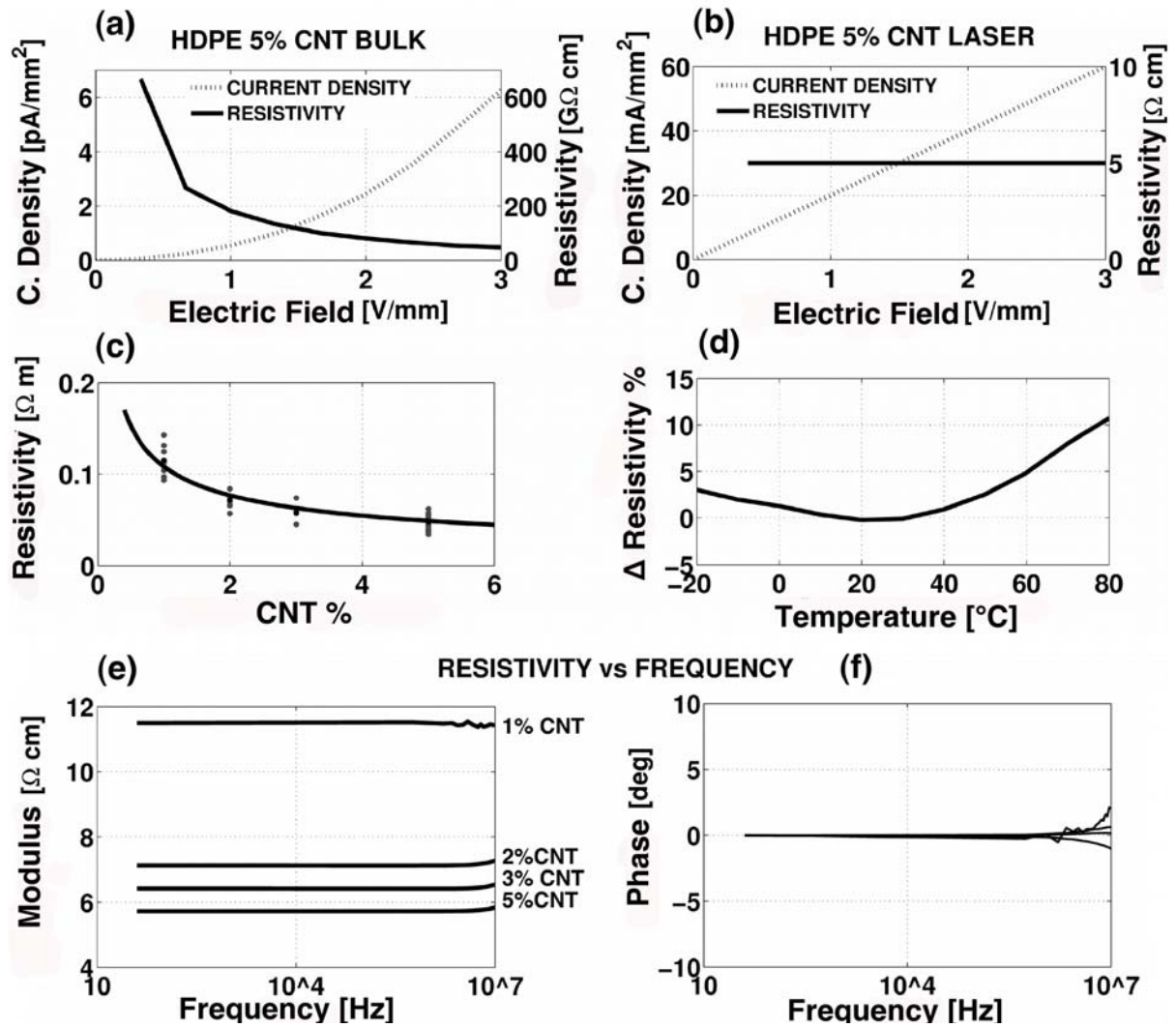
Fig. 6. Electrical properties of HDPE-CNT composite. (a) DC characteristic of the untreated *5 wt%* CNT composite, (b) DC characteristic of the irradiated 5 wt% CNT composite, (c) Effect of the filler concentration on the resistivity of the irradiated composite, (d) Effect of the temperature on the resistivity of the irradiated composite (e) Modulus of the AC characteristic of the irradiated composite (f) Phase of the AC characteristic of the irradiated composite. The modulus here, is the absolute value of the complex electrical resistivity (also called impeditivity), which is calculated by sqrt(R_e^2+I_m^2), where R_e is the real part of the resistivity and I_m the imaginary part.

Fig. 6c shows that the effect of irradiation is only weakly dependent on the filler concentration. The resistivity decreases linearly with the filler concentration through an exponent *t* around *t=-0.497±0.042*. Data comprised in the *-3.54<t<-1.77t* interval are reported for non-irradiated CNT-PE composites (Supplementary data) [35-37]. From an industrial point of view, this feature has the advantage to allow a control of the conductivity of the composite only by adjusting the irradiation parameters.

Fig. 6d shows the effect of the temperature on the resistivity of the irradiated composite: the resistivity increases up to *12%* in the *30–80 °C* interval, is stable in the *20–30 °C* interval and decreases up to *3%* in the *-20–20°C* range. A very similar behavior was described for CNT buckypaper.[38] Either negative (NTC) or positive temperature coefficient (PTC) [37, 39, 40] have been reported for non-irradiated CNT-PE (Supplementary data).

The dependence of the complex AC resistivity upon frequency is presented in Fig. 6e,f: the modulus and the phase of the complex resistivity are independent on the frequency in all the considered range up to *10 MHz*. Therefore the sample can be assimilated to a resistor, with a pure Ohmic behavior and low dielectric constant. Comparison with literature data shows that the AC behavior of the irradiated composite is similar to that of the untreated composites with high filler concentration [31, 36, 39, 41]. In conclusion, the irradiation is modifying the AC electrical character of the composite from dielectric to metallic behaviour.

As the electric properties depend on the CNT contacts in the percolated area, we expect that the conductivity can depend upon the deformation (i.e. piezoresistivity). To confirm this hypothesis, preliminary and qualitative experiments on the effects of the mechanical deformation on the conductivity have been performed on 3wt% sample A practical application of our conductive tracks, based on conductivity and on piezoresistive effects, is shown in a movie (Supplementary data).

4. Conclusions

The fabrication of metal-free conductive tracks, firmly adhering on the surface of HDPE/MWCNT composites, by means of a laser stimulated localized percolation of carbon nanotubes is illustrated. The IR-based laser beam, being strongly absorbed by the carbon nanotubes, causes the local melting of the composite with formation of v-shaped channels. The concentration of MWCNTs in the external layer of the walls of the v-shaped tracks increases overcoming the percolation concentration even on low concentrated samples, with subsequent increase of conductivity by several orders of magnitude with respect to the bulk material. The structure of conductive paths has been imaged by SEM, by charge contrast low-voltage SEM, AFM and conductive AFM. It is demonstrated that the track conductivity is only weakly dependent upon the filler concentration. The adopted laser printing manifold allows fast writing of complex patterns, a fact which makes the process interesting from the industrial point of view. The conductive tracks formed by the printing procedure being surrounded by a insulating material (with CNT concentration below the electric percolation threshold) can have potential use in many application fields for electrical signals transport. Preliminary results obtained on the 1-5wt% samples also shows that the conductive tracks

have piezoresistive properties and can so have applications as pressure sensors (Supplementary data and video).

References

[1]   Balazs AC, Emrick T, Russell TP. Nanoparticle Polymer Composites: Where Two Small Worlds Meet. *Science* 2006 November 17, 2006; 314(5802):1107-10.

[2]   Ma PC, Siddiqui NA, Marom G, Kim JK. Dispersion and functionalization of carbon nanotubes for polymer-based nanocomposites: A review. *Composite Part A-Appl Sci Manuf* 2010; 41(10):1345-67.

[3]   Verdejo R, Bernal MM, Romasanta LJ, Lopez-Manchado MA. Graphene filled polymer nanocomposites. *J Mater Chem* 2011; 21(10):3301-10.

[4]   Zhang RW, Moon KS, Lin W, Agar JC, Wong CP. simple and effective way to prepare highly conductive polymer composites by in situ reduction of silver carboxylate. *Compos Sci Technol* 2011; 71(4):528-34.

[5]   Guldi DM. Materials science - Nanotubes see the light. *Nature* 2007; 447(7140):50-1.

[6]   Qian H, Greenhalgh E, Shaffer M, Bismarck A. Carbon nanotube-based hierarchical composites: a review. *J Mater Chem* 2010; 20(23):4751-62.

[7]   Chun K-Y, Oh Y, Rho J, Ahn J-H, Kim Y-J, Choi HR, et al. Highly conductive, printable and stretchable composite films of carbon nanotubes and silver. *Nat Nanotechnol* 2010 Dec 2010; 5(12):853-7.

[8]   Ajayan PM, Stephan O, Colliex C, Trauth D. Aligned carbon nanotube arrays formed by cutting a polymer resin-nanotube composite. *Science* 1994; 265(5176):1212-4

[9]   Cesano F, Bertarione S, Scarano D, Zecchina A. Connecting carbon fibers by means of catalytically grown nanofilaments: Formation of carbon-carbon composites. *Chem Mater* 2005; 17(20):5119–23.

[10]   Rahman MM, Cesano F, Bardelli F, Scarano D, Zecchina A. Hybrid SnO_2/carbon composites: From foams to films by playing with the reaction conditions. *Catal Today* 2010; 150(1):84-90.

[11]   Mamedov AA, Kotov NA, Prato M, Guldi DM, Wicksted JP, Hirsch A. Molecular design of strong single-wall carbon nanotube/polyelectrolyte multilayer composites. *Nat Mater* 2002; 1(3):190-4.

[12]   Kaiser AB, Skakalova V. Electronic conduction in polymers, carbon nanotubes and graphene. *Chem Soc Rev* 2011; 40(7):3786-801.

[13]   Spitalsky Z, Tasis D, Papagelis K, Galiotis C. Carbon nanotube–polymer composites: Chemistry, processing, mechanical and electrical properties. *Prog Polym Sci* 2010; 35(3):357-401.

[14]   van Osch THJ, Perelaer J, de Laat AWM, Schubert US. Inkjet Printing of Narrow Conductive Tracks on Untreated Polymeric Substrates. *Adv Mater* 2008; 20(2):343-5.

[15]   Kordas K, Mustonen T, Toth G, Jantunen H, Lajunen M, Soldano C, et al. Inkjet Printing of Electrically Conductive Patterns of Carbon Nanotubes. 2006; 2(8-9):1021-5.

[16]   Gao W, Singh N, Song L, Liu Z, Reddy ALM, Ci L, et al. Direct laser writing of micro-supercapacitors on hydrated graphite oxide films *Nat Nanotechnol* 2011; 6(8):496-500.

[17]   Cho J, Shin K-H, Jang J. Micropatterning of conducting polymer tracks on plasma treated flexible substrate using vapor phase polymerization-mediated inkjet printing. *Synth Met* 2010; 160(9-10):1119-25.

[18]   Putsch P. *Fakuma – International Trade Fair for Plastics Processing, Hall A7, Stand 7214*. Friedrichshafen 2008.

[19]   Putsch P, inventor PP-MID GMBH, assignee. Polymer molded bodies and printed circuit board arrangement and method for the production thereof Germany patent PCT/EP2009/005757. 2009 11/02/2010.

[20]   Cravotto G, Garella D, Turci F, Calcio Gaudino E, Bertarione S, Agostini G, et al. Rapid purification/oxidation of multi-walled carbon nanotubes under 300 kHz-ultrasound and microwave irradiation. *New J Chem* 2011; 35(4):915-9.

[21]   Gavello D, Vandael D, Cesa R, Premoselli F, Marcantoni A, Cesano F, et al. Altered excitability of cultured chromaffin cells following exposure to multi-walled carbon nanotubes. *Nanotoxicology* 2012; 6(1):47-60.

[22]   Olley RH, Bassett DC. An improved permanganic etchant for polyolefines. *Polymer* 1982; 23(12):1707-10.

[23]   Antunes EF, Lobo AO, Corat EJ, Trava-Airoldi VJ, Martin AA, Veríssimo C. Comparative study of first- and second-order Raman spectra of MWCNT at visible and infrared laser excitation. *Carbon* 2006; 44(11):2202–11.

[24]   Lehman JH, Terrones M, Mansfield E, Hurst EK, Meunier V. Evaluating the characteristics of multiwall carbon nanotubes. *Carbon* 2011; 49(8):2581–602.

[25]   Cesano F, Groppo E, Bonino F, Damin A, Lamberti C, Bordiga S, et al. Polyethylene Microtubes from Silica-Fiber-based Polyethylene Composites Synthesized by Using an In Situ Catalytic Method. *Adv Mater* 2005; 18(23):3111–4.

[26]   Sato H, Shimoyama M, Kamiya T, Amari T, Šašic S, Ninomiya T, et al. Raman spectra of high-density, low-density, and linear low-density polyethylene pellets and prediction of their physical properties by multivariate data analysis. *J Appl Polym Sci* 2002; 86(2):443–8.

[27]   Kowalska P, Cheeseman JR, Razmkhah K, Green B, Nafie LA, Rodger A. Experimental and Theoretical Polarized Raman Linear Difference Spectroscopy of Small Molecules with a New Alignment Method Using Stretched Polyethylene Film. *Anal Chem* 2012; 84(3):1394–401.

[28]   Teng CC, Ma CCM, Huang YW, Yuen SM, Weng CC, Chen GH, et al. Effect of MWCNT content on rheological and dynamic mechanical properties of multiwalled carbon nanotube/polypropylene composites. *Composite Part A-Appl Sci Manuf* 2008 Dec; 39(12):1869-75.

[29]   Villmow T, Pegel S, Potschke P, Wagenknecht U. Influence of injection molding parameters on the electrical resistivity of polycarbonate filled with multi-walled carbon nanotubes. *Compos Sci Technol* 2008 Mar; 68(3-4):777-89.

[30]   Valentino O, Sarno M, Rainone NG, Nobile MR, Ciambelli P, Neitzert H, et al. Influence of the polymer structure and nanotube concentration on the conductivity and rheological properties of polyethylene/CNT composites 2008; 40(7):2440-5.

[31]   Li W, Bauhofer W. Imaging of CNTs in a polymer matrix at low accelerating voltages using a SEM. *Carbon* 2011; 49(12):3891-8.

[32]   Cesano F, Pellerej D, Scarano D, Ricchiardi G, Zecchina A. Radially organized pillars in TiO_2 and in TiO_2/C microspheres: Synthesis, characterization and photocatalytic tests *J Photochem Photobiol - A Chem* 2012; 242( ):51-8.

[33]   Liu CH, Fan SS. Nonlinear electrical conducting behavior of carbon nanotube networks in silicone elastomer *Appl Phys Lett* 2007; 90(4):041905-8.

[34]   Gau C, Kuo C-Y, Ko HS. Electron tunneling in carbon nanotube composites. *Nanotechnology* 2009; 20(39):395705.

[35]   Mierczynska A, Mayne-L'Hermite M, Boiteux G, Jeszka JK. Electrical and mechanical properties of carbon nanotube/ultrahigh-molecular-weight polyethylene composites prepared by a filler prelocalization method. *J Appl Pol Sci* 2007; 105(1):158-68.

[36]   Lisunova MO, Mamunya YP, Lebovka NI, Melezhyk AV. Percolation behaviour of ultrahigh molecular weight polyethylene/multi-walled carbon nanotubes composites *Eur Pol J* 2007; 43(3):949-58.

[37]   Jeon K, Lumata L, Tokumoto T, Steven E, Brooks J, Alamo R. Low electrical conductivity threshold and crystalline morphology of single-walled carbon nanotubes-high density polyethylene nanocomposites characterised by SEM, Raman spectroscopy and AFM. *Polymer* 2007; 48(16):4751-64

[38]   Chen I-WP, Liang R, Zhao H, Wang B, Zhang C. Highly conductive carbon nanotube buckypapers with improved doping stability via conjugational cross-linking. *Nanotechnology* 2011; 22(48):485708.

[39]   He XJ, Du JH, Ying Z, Cheng HM. Positive temperature coefficient effect in multiwalled carbon nanotube/high-density polyethylene composites. *Appl Phys Lett* 2005; 86(6):062112.

[40]   Liang GD, Tjong SC. Electrical properties of low-density polyethylene/multiwalled carbon nanotube nanocomposites. *Mater Chem Phys* 2006; 100(1):1-5.

[41]   Logakis E, Pandis C, Peoglos V, Pissis P, Pionteck J, Pötschke P, et al. Electrical/dielectric properties and conduction mechanism in melt processed polyamide/multi-walled carbon nanotubes composites. *Polymer* 2009; 50(21):5103–11.

Structure and properties of metal-free conductive tracks on polyethylene/multiwalled carbon nanotube composites as obtained by laser stimulated percolation

Federico Cesano[a§], Ismael Rattalino[b§], Danilo Demarchi[b], Fabrizio Bardelli[a], Alessandro Sanginario[b], Annamaria Gianturco[c], Antonino Veca[c], Claudio Viazzi[d], Paolo Castelli[d], Domenica Scarano[a], and Adriano Zecchina[a]*

[a] Department of Chemistry and NIS (Nanostructured Interfaces and Surfaces) Centre of Excellence and INSTM Centro di Riferimento, University of Torino, Via P. Giuria, 7, 10125 Torino (Italy);
[b] Department of Electronics and Telecommunications, Politecnico di Torino, Corso Duca degli Abruzzi 24, 10129 Torino (Italy);
[c] Centro Ricerche Fiat S.C.p.A., Str. Torino 50, I-10043 Orbassano (Italy);
[d] RTM Laser Technology SpA, Via Circonvallazione 10, I-10011 Agliè (Italy);
[§] these authors contributed equally to this work.

Supplementary Data
The structure of the composite after laser irradiation.

The structure of the laser irradiated MWCNT/polymer composites is shown in Fig. S 1a-c, respectively. From these SEM lateral views it is evident that the thermal treatment of the laser beam causes a v-shape track in the irradiated region for all samples.

Cross-sections of the laser irradiated MWCNT/polymer composites with 1wt%, 3wt% and 5wt% of CNTs are shown in Figure S 2a-c, respectively. The depth of the v-channels is decreasing by increasing the concentration of CNTs from 1wt% to 5wt%.This effect is due to the thermal conductivity which increases in the same order. In all cases a percolation layer is clearly observed (Fig. S 2).
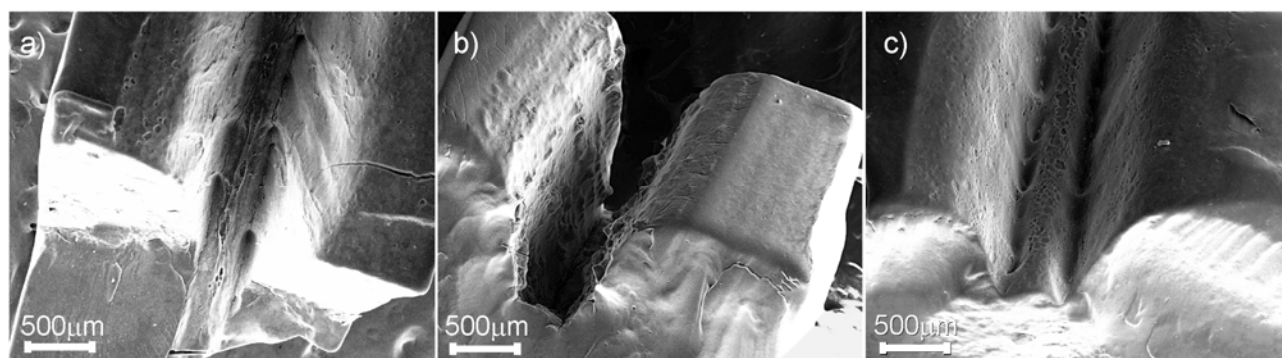
Fig. S 1. SEM lateral views of CNT/HDPE composites in the laser irradiated regions: a) 1 wt%, b) 3 wt% and c) 5 wt% of MWCNTs.
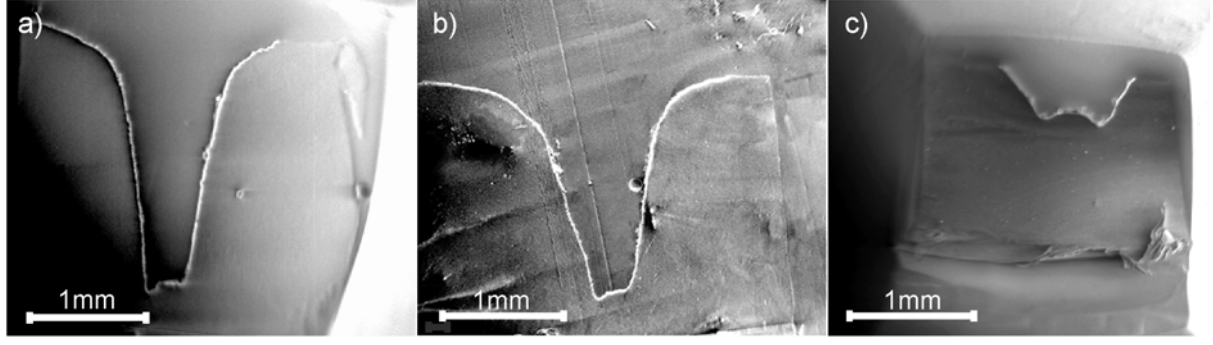
Fig. S 2. SEM cross sections of the laser irradiated areas of CNT/HDPE composites: a) 1 wt%, b) 3 wt% and c) 5wt % of MWCNTs, as obtained by means of secondary electrons in charge contrast imaging mode under low acceleration voltage (0.3 KeV) to gain surface potentials [26, 27]. To reduce the edge effects, the samples (bottom part) were embedded in a epoxy resin and cut with a diamond knife by ultramicrotome technique. Dark-grey regions refer to non-conductive region (epoxy resin) or CNTs/HDPE portions below the percolation threshold, whereas the bright regions refer to the electric conductive areas.

Scaling procedure.

The scaling operation is useful to compare the electrical properties of samples with different geometrical dimensions and can be summarized by the well-known formula:

$$\frac{V}{l} = \rho \, \frac{I}{A} \, , \qquad V = \rho \, \frac{l}{A} \, I \, , \qquad V = R \, I \tag{1}$$

Where I is the current, V the voltage, V/l the average electric field, I/A the current density, ρ the resistivity and R the resistance. The transport section A of the irradiated composites was estimated from the SEM images shown, which were acquired in charge contrast imaging mode. The transport section is the bright transversal surface of the image, which can be easily identified with respect to the black not conductive background.

Regression procedure.

The expression of the regression and the values of parameters are:

$$\log_{10} \rho = t \log_{10} \phi + \log_{10} \rho_0 \ , \qquad \frac{\rho}{\rho_0} = \phi^t \qquad (2)$$

$$t = -0.497 \pm 0.042 \ , \qquad \rho_0 = 10^{-0.966 \pm 0.048} \ , \qquad R^2 = 0.814 \qquad (3)$$

Where t is the slope of the line in the double logarithmic space and ρ_0 an adjustable parameter. R^2 is the coefficient of determination, which gives the goodness of the fitting as a number between *0* (no significance) and *1* (optimal significance). We performed the Kolmogorov-Smirnov test on the statistical distribution of data, obtaining that a normal distribution is acceptable with an error of the first kind of *10%*. The confidence intervals of t and ρ_0 are obtained by assuming a normal distribution, with a confidence level of *68%* (1 standard deviation from the mean).

AC electrical analysis.

In AC electrical regime, it is convenient to consider the conductivity as a complex quantity, in general given by the following expressions [37]:

$$\sigma_c = \frac{1}{\rho_r} + j\omega\epsilon \ , \qquad \sigma_c = |\sigma_c| e^{j \times phase(\sigma_c)} \qquad (1)$$

$$|\sigma_c| = \sqrt{\frac{1}{\rho_r{}^2} + \omega^2\epsilon^2} \ , \qquad phase(\sigma_c) = \arctan(\omega\epsilon\rho_r)| \qquad (2)$$

Where ρ_r is the DC resistivity and ϵ is the absolute dielectric constant. The complex resistivity is the inverse of complex conductivity and it is given by:

$$\rho_c = \frac{1}{|\sigma_c|} e^{-j \times phase(\sigma_c)} \qquad (3)$$

These expressions fit very well the case of CNT-polymer composites, which can be electrically modelled by the parallel between a resistance R and a capacitance C [38]. The resistance R models the intrinsic resistivity of CNTs, the capacitance C models the dielectric effect of the polymeric chains between CNTs. The resulting admittance is given by:

$$Y = \frac{1}{R} + j\omega C = \left(\frac{1}{\rho_r} + j\omega\epsilon\right)\frac{A}{l} = \sigma_c \frac{A}{l} \qquad (4)$$

Where A is the transversal area and l the length of the sample. Equation 4 shows that the admittance of an RC parallel is equal to the expression of the conductivity, except for the geometric scaling factor A/*l*.

By applying the basic electric circuit theory, it is simple to verify that this model predicts a cut off frequency f_c for the resistivity around $1/(2\pi RC) = \sigma_r/(2\pi\varepsilon)$ Hz [37]. The theory predicts a modulus increase of 29 % and a phase rotation of 45° at the cut off frequency. This equivalent circuit is confirmed for polymer-CNT composites [36, 39], as long as the non linearity of the circuit is taken into account. The non linearity arises from the dependence of the real and imaginary parts of σ_c on the amplitude of the applied voltage and it can be corrected by adding some proper coefficients in the classical circuit theory. The following equation resumes the classical circuit theory and the correction needed for polymer-CNT composites.

$$|\sigma_c| = \begin{cases} \sigma_r, & \text{if } f \to 0 \ (f < f_c) \\ \epsilon(2\pi f)^s, & \text{if } f \to +\infty \ (f > f_c) \\ s = 1, & \text{in the linear circuit theory} \\ 0 < s < 1, & \text{in polymer-CNT composites [3–5]} \end{cases} \tag{5}$$

For the phase a similar expression can be provided, where it is around 0° before $f_c/10$ and starts increasing over $f_c/10$. Equation 5 shows that the cut off frequency f_c ideally separates the electric response into two different ranges of frequency. This is a typical behavior for a wide variety of materials and it is called by Jonscher "universal dynamic response" (UDR) [40]. Both the correction exponent s and the cut off frequency generally depend on the voltage, the temperature and the filler concentration. ε is not properly the dielectric constant for s≠1, but a fitting parameter still connected to the dielectric response.

The effect of the concentration of CNTs and of temperature.

The values of t are much higher than our value, which means that an increase of the filler concentration affects more the conductivity of the untreated composite than that of the irradiated one.

Possible explanation of the curve in Figure 5d takes into account the effects due to the filler and to the matrix separately. In general, similarly to semiconductors [41], an increase of temperature induces a decrease of CNT resistivity, whereas the simultaneously thermal expansion of the matrix increases the overall resistivity inducing the breakdown of the original conductive network by CNT physical separation [34]. Under cooling, the thermal contraction of the polymer does not considerably affect the filler network, since the connections among CNTs are already established.

AC resistivity upon frequency.

In general, the AC electrical model of CNT-polymer composites is a R-C parallel [38], where the resistance R models the intrinsic resistivity (ρ) of the CNT network and the capacitance C models the dielectric constant (ε) of the polymer. This model determines a cut off frequency f_c for the resistivity around $1 / (2\pi RC) = 1/(2\pi\rho\varepsilon)$, which ideally separates the electric response into two different ranges of frequency: under f_c the modulus is independent from the frequency and the phase is around $0°$, over f_c the modulus decreases and the phase turns from $0°$ [36, 41]. The cut off frequency was observed in PE-CNT composites around $1\ kHz$ for a filler concentration of 3.6 wt% [32]. An increase of the filler concentration reduces R and C through the relative addition of the conductive phase with respect to the dielectric matrix, thus resulting not only in an increase of DC conductivity but also in a shift of the cut off frequency towards higher frequencies [32, 36, 41]. Over a certain filler concentration, the cut off frequency shifts over the full scale of the instrument, so that the resistivity appears independent from the frequency and the phase around $0°$.

Conductive/piezoresistive measurements prototyping.

In the set-up the conductivity variation induced by the finger pressure on tracks 3 cm long, is measured (Fig. S3).
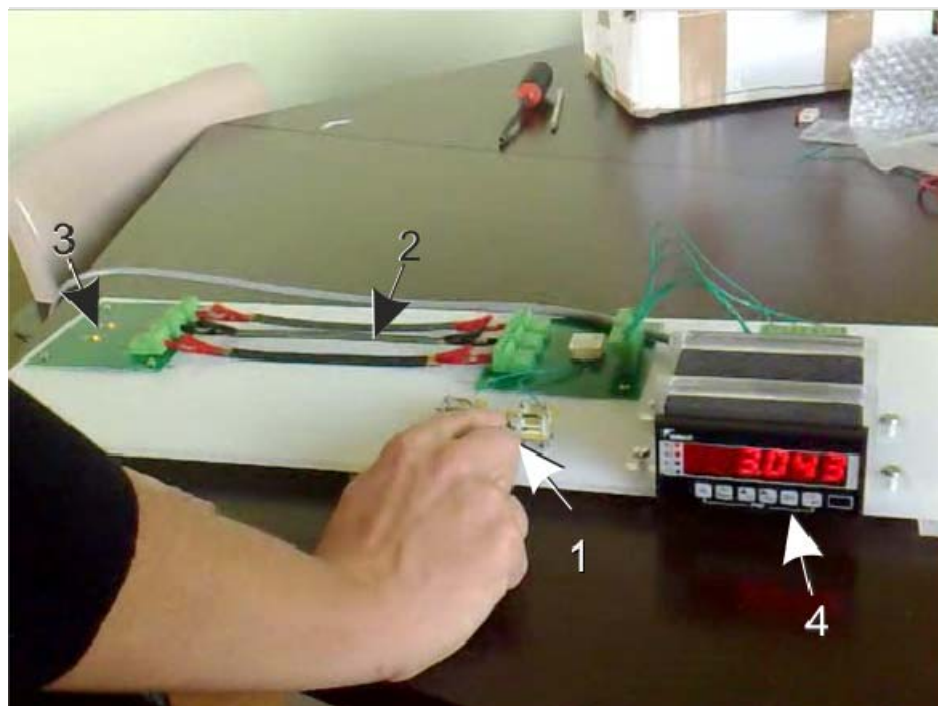
Fig. S 3. A prototype made of an electric circuit connected to strips of material (HDPE/MWCNT composites, 3 wt% CNTs) laser-irradiated: (1) tracks 3 cm long, working as

switching button upon deformation (piezoresistive properties), (2) tracks of 10 cm working as conductors, (3) light-emitting diodes (LEDs) and (4) the measured resistance of the conducting tracks (KOhms).

Other references:

[37]   McLachlan, D. S.; Sauti, G., *Journal of Nanomaterials* **2007**, 30389-30397.

[38]   Hsu, W. K.; Kotzeva, V.; Watts, P. C. P.; Chen, G. Z., *Carbon* **2004,** 42, 1707-1712.

[39]   He, L. X.; Tjong, S. C., *The European Physical Journal E* **2010,** 32, 249-254.

[40]   Jonscher, A. K., *Nature* **1977,** 267, 673-679

[41]   Fujita, S.; Suzuki, A., *Journal of Applied Physics* **2010,** 107, 013711-14.